Power Performance Analysis in Off-Grid Photovoltaic Battery System with ANFIS-FL Based MPPT Under Partial Shading Effects

A. Boudaoud*, M. A. Atillah, H. Stitou, M. Aqil

Engineering and Applied Physics Team (EAPT), Superior School of Technology, Sultan Moulay Slimane University, Beni Mellal, Morocco

ABSTRACT: Photovoltaic (PV) systems combined with battery storage offer a reliable and autonomous energy solution for isolated regions. However, ensuring an optimal energy balance between production and consumption, while maintaining system stability under variable solar irradiation, remains a significant challenge. Therefore, the study proposes an all-encompassing control system for off-grid photovoltaic (PV) systems. The approach considers an MPPT algorithm with adaptive neuro-fuzzy inference system (ANFIS) and fuzzy logic (FL) as the controller, which would maximize energy extraction from photovoltaic panels subjected to partial shading conditions. The system also includes a DC-AC inverter with vector control to maintain the DC bus voltage at 800 V, together with a battery management algorithm to supervise battery charging and discharging. Energy dissipation is also incorporated to balance excess production. The system's performance was simulated and evaluated using two constant loads: 35 KW and 40 KW. Results highlight a critical operational distinction: while the 40 KW scenario was fully managed by the battery storage capabilities, the 35 KW scenario required the active intervention of the dissipation system to evacuate excess power and maintain DC bus stability. Simulation results demonstrate that the proposed ANFIS-FL controller achieves a rapid MPPT response time of 0.05 s, successfully tracking the Global Maximum Power Point (GMPP) under dynamic partial shading without steady-state oscillations. Regarding stability, the DC bus voltage was tightly regulated at 800 V, with transient overshoots limited to 6.25% and 9% under the 35 KW and 40 KW scenarios, respectively.

***KEYWORDS*:** MPPT, ANFIS, Fuzzy Logic, Off-Grid, Photovoltaic, Battery, Partial shading.

[Received May 05, 2025; Revised Dec. 05, 2025; Accepted Dec. 21, 2025] Print ISSN: 0189-9546 | Online ISSN: 2437-2110

I. INTRODUCTION

The electricity supply to isolated areas or those far from conventional grids is one of the key provisions of off-grid PV systems. They create clean energy at low cost by tapping the ever-renewable resource, the sun (Kelly et al., 2023). Under any circumstance, these installations have to assure maximum reliability since electricity would have to be supplied to the consumer on an autonomous basis without sun power, and this is achieved through the use of batteries or other energy-storing devices (Mokhtara et al., 2021). To manage the power flows of the off-grid system involves the distribution of power produced by the solar panels in such an efficient manner as to ensure that production, consumption, and storage remain balanced at all times. Stability within the system is largely dependent on the capability to manage these energy flows dynamically and in real time, especially with the variation of solar irradiation (Ghizlane et al., 2024). Naturally, acceptable methods employed for optimizing solar energy power generation become yet another challenge-an auxiliary threat to maximizing power delivery by solar panels. Solar PV panels rarely operate at full power because of solar irradiation, ambient temperature, and weather conditions (Atillah et al., 2023). With respect to these variations, an MPPT is introduced to track and extract the maximum power from that which is delivered by the solar panels. But a recurrent problem afflicting those new solar installations is partial shading, where obstacles partially shade one or more of the solar panels either by nature or by man. It is because partially shading the array that such a great limitation is placed on the MPPT system in being able to find and hold the maximum power point, thus degrading the performance of the overall system.

Several researchers have contributed to the evaluation of off-grid systems. From Yatimi et al., an overview has been presented on their study about off-grid PV modeling and control in which they considered a system with an MPPT algorithm based on backstepping (Yatimi et al., 2020). Whereas in Chtita et al.'s study, a control strategy to adjust the energy balance was put forth while charging batteries with solar energy for off-grid PV systems (Chtita et al., 2021). Such methods, though effective in principle, often cannot operate under non-ideal conditions. Indeed, according to more recent papers, conventional algorithms cannot follow the global MPP when subjected to partial shading conditions, under which performance is heavily degraded (Timur and Uzundağ, 2025) (Çakmak et al., 2025). Further, Rad et al. have given an analysis of the

*Corresponding author: abdelghani.boudaoud@usms.ma ***doi:*** http://doi.org/10.63746/njtd.v22i5.3640

issue of electricity surplus in hybrid systems and how it affects stability and reliability (Rad et al., 2023). Assem et al., on the other hand, have innovatively brought adaptive control using fuzzy logic and power supervision for PV-battery systems into contention (Assem et al., 2023). As mentioned earlier, the fuzzy logic has gone on to become a prevalent approach. Some of the studies propose fuzzy controllers in solar battery chargers that not only do MPPT but also voltage regulation so that batteries are charged safely and efficiently (Seguel et al., 2025).

Despite the abundance of literature on off-grid PV systems, a critical gap remains regarding the stability of integrated architectures under dynamic partial shading conditions. Existing solutions typically exhibit a dichotomy:

- Standard Integrated Systems: Often rely on conventional MPPT algorithms (like P&O) to simplify control. While stable under uniform irradiation, these systems fail to track the Global MPP during partial shading, leading to significant energy loss and voltage ripples that stress the battery.
- Advanced MPPT Studies: Research focusing on intelligent algorithms (PSO, ANN) often validates tracking efficiency in isolation. These studies frequently neglect the system-level transient analysis, failing to quantify how rapid tracking adjustments impact DC bus stability and battery current stress during shading transitions.

Consequently, there is a lack of comprehensive studies that bridge this gap by combining a robust hybrid intelligent controller (ANFIS-FL) with a rigorous analysis of the entire energy conversion chain. Specifically, the inadequacy of current literature lies in ensuring simultaneous global peak tracking and transient voltage/current mitigation without imposing excessive computational burdens. In light of these limitations, the core research problem lies in the lack of an integrated control framework that can effectively handle the non-linearity of partial shading without relying on excessive training data or computational complexity, while simultaneously ensuring stable battery management.

Our research differentiates itself by instilling a recent hybrid MPPT methodology that considers the ANFIS in finding the voltage corresponding to the MPP for given sunlight inputs and combines it with the fuzzy logic (FL) controller acting as a PI controller to hold that output voltage of the PV. The significance of ANFIS for MPPT has been proven by its very high accuracy (Khan et al., 2023) but suffers a major weakness in that it requires thorough training data so that it does not converge on a local maximum if partial shading exists (Mohammed et al., 2025). Our hybrid approach, whose effectiveness is corroborated by recent comparative studies (Atillah et al., 2024), is exactly intended to tackle that problem. Another highlight of this article is the examination of this MPPT method under partial shading conditions, which is a significant addition to the literature, as most MPPT strategies, including those based on ANFIS, are not yet mature enough to fully integrate this aspect. While previous studies have focused on specific parts of the system, Chtita et al. on battery management (Chtita et al., 2021), Rad et al. on surplus energy management (Rad et al., 2023), and Yatimi et al. on MPPT (Yatimi et al., 2020), this study aims to make integrated advances that treat these three areas as interdependent.

This paper explores the design of an alternative off-grid energy solution, powered by PV panels, with the integration of an ANFIS-based MPPT with an FL controller whose role is to maintain the PV panel's output voltage at the MPP voltage determined by the ANFIS model. This allows the power generated by the PV panel to be maximized under varied conditions, even in partial shading. At the same time, a battery-based storage system is incorporated, managed by a bidirectional buck-boost converter, and controlled by a management algorithm to ensure safe and optimal charging/discharging of the batteries. To guarantee a stable power supply, a DC-AC inverter with a filter is used, ensuring DC bus voltage regulation via a dedicated control. Within this architecture, three-phase resistive loads are connected. A crucial aspect of the design is the evacuation of excess power to a resistor connected to the DC bus. This strategy maintains the system's power balance.

The article is organized as follows: section 2 describes the methodologies and materials, while section 3 discusses the results. The conclusion is in section 4.

II. MATERIALS AND METHODS

The system adopted in this work is divided into four main parts:

- First part: PV with MPPT control applied to the DC-DC boost converter.
- Second part: DC-AC inverter with control to regulate the DC bus voltage.
- Third part: Battery and a charge/discharge control algorithm.
- Fourth part: Dissipating excess energy.

This study will focus on the MPPT method and management of energy flows, both on the storage side and on the dissipation side of excess energy. Fig. 1 presents the global structure of the system in MATLAB Simulink.

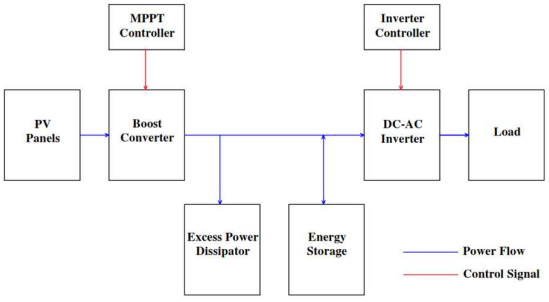

Fig. 1 Synoptic block diagram of the proposed off-grid system architecture

A. MPPT control

The PV panel used in this study is shown in Fig. 2 We assembled three groups of panels in series to obtain a

total output of around 50 KW at an irradiance of 1000 W/m².
Fig. 3(a) and Fig. 3(b) show the electrical characteristic of the PV used, representing power as a function of voltage for a constant temperature of 25°C. This curve has been plotted for different irradiation values; to show the evolution of the power delivered by the panel under various sunlight conditions, whether uniform irradiation or partial shading.

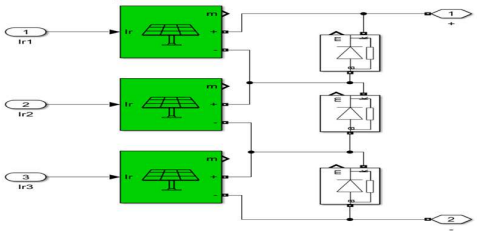

Fig. 2. PV panel used

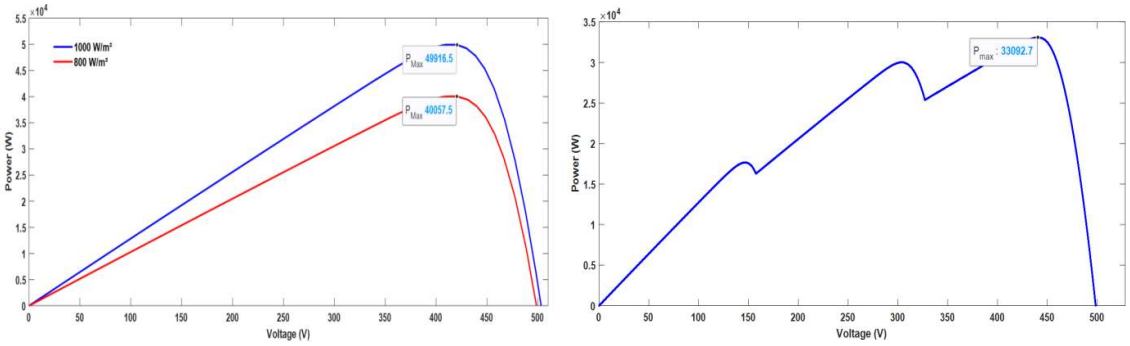

(a) (b)

Fig. 3 (a) Electrical characteristics under uniform irradiance (b) Electrical characteristics at partial shading

According to the panel's characteristics, under uniform irradiation conditions, It should provide a maximum power of approximately 50 KW when the irradiation is 1,000 W/m². When irradiation is reduced to 800 W/m², the maximum power expected is around 40 KW, while under conditions of partial shading, where each group of panels receives different irradiation, the maximum total power supplied by the system is around 33 KW.

1) MPPT based on ANFIS–FL Principle

This section presents the principle of the MPPT method based on ANFIS and FL controller, as illustrated in Fig. 4. This approach relies on two key components: an ANFIS model and a fuzzy controller, which work in synergy to optimize the performance of the PV system.
The ANFIS model processes solar irradiation and temperature as inputs to generate the voltage reference that matches the maximum power point. The FL controller plays a complementary role by maintaining the system's operation at the MPP voltage provided by the ANFIS model. Acting as a proportional-integral regulator, the FL controller adjusts the DC-DC boost converter duty cycle in real-time. The choice of a fuzzy logic controller is particularly suited to this application because the small-signal model of a PV system with the boost converter is non-linear (Zhang and Zhang, 2019). Unlike conventional controllers that require an accurate mathematical model, the FL controller relies on general system knowledge and heuristic rules, allowing it to operate efficiently in non-linear and time-varying environments. In our study, the temperature was kept constant, and only the solar irradiance was modified to evaluate the system's performance.

To simulate uniform irradiation conditions, two different irradiation levels were applied to the three panels of the installation. First, an irradiance of 1000 W/m² was applied simultaneously to all panels. Then, an irradiance of 800 W/m² was applied to all panels to simulate a decrease in solar irradiance. For partial shading simulation, every panel group received a different irradiance: 1000 W/m² for the first group, 800 W/m² for the second, and 600 W/m² for the third. This situation represents a realistic scenario where obstacles or shadows affect part of the panels, creating a non-uniform distribution of irradiation (Atillah et al., 2024).

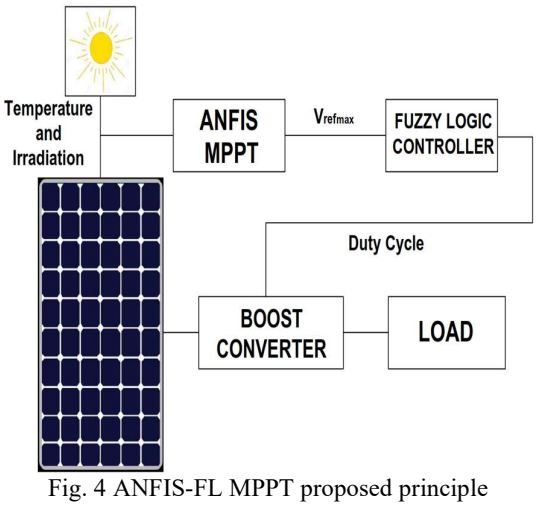

Fig. 4 ANFIS-FL MPPT proposed principle

ANFIS associates artificial neural networks with FL to improve modelling and the making of decisions in complex systems (Chapala et al., 2024). By using the capability of neural networks to learn and recognize

models from data, and applying the principles of FL to manage uncertainty and imprecision, ANFIS offers an efficient method for converting input signals into exact outputs. This adaptive process adjusts the parameters of the fuzzy inference system using machine learning algorithms, enabling continuous performance optimization (Mohammed et al., 2024). The ANFIS architecture is detailed in (Stitou et al., 2024).

2) Conception of ANFIS-FL MPPT

To build the ANFIS model, we used the neuro-fuzzy design tool available in the MATLAB environment (Farah et al., 2020), as illustrated in Fig. 5. This tool enables a neuro-fuzzy inference system to be built and trained, by defining the parameters of the ANFIS model, such as input and output variables, the number of membership functions, as well as learning methods, etc. The designer then performs a training run on the ANFIS model. The designer then learns from the training data, adaptively adjusting the system parameters to achieve optimum accuracy (Aghdam et al., 2024). This facilitates the modeling of complex relationships between variables, enabling the efficiency of the MPPT method to be maximized under different irradiation conditions.

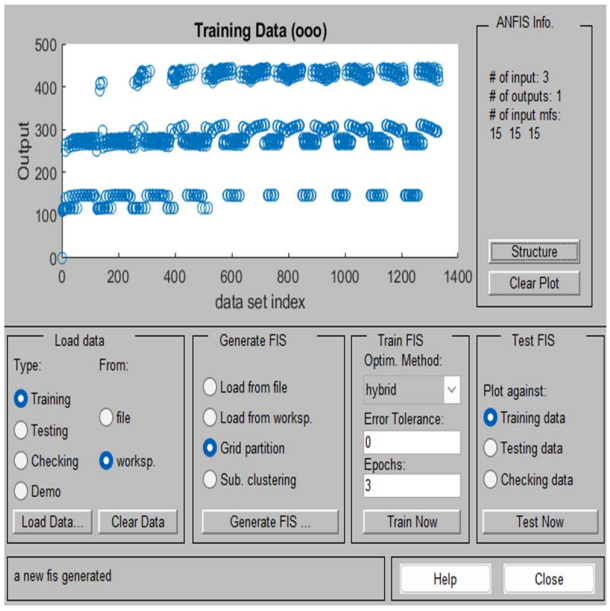

Fig. 5 ANFIS MATLAB designer

To train the ANFIS model effectively, a comprehensive dataset consisting of 1400 input-output pairs was generated using the mathematical model of the PV array in MATLAB. The dataset covers the entire operating range, including uniform irradiation and severe partial shading scenarios, to ensure the model's generalizability. Table 1 presents a representative extract of 10 samples from this dataset to illustrate the diversity of training cases. The inputs correspond to the irradiance levels of the three PV modules, while the target output is the theoretical optimal voltage (V_{mpp}) calculated for each specific shading pattern.

Table 1 Training data selection

Irradiation Pv1	Irradiation Pv2	Irradiation Pv3	Voltage of MPP
1000	1000	1000	415.49
800	600	100	304.90
800	100	100	146.76
100	800	100	146.76
300	600	500	271.92
400	700	1000	274.70
900	400	600	441.89
600	300	400	435.41
400	800	900	269.30
200	800	800	266.48

The adopted configuration for the ANFIS model is as follows: the membership function type is triangular, with 15 membership functions (MF) for the three inputs and 3 epochs. The results are encouraging; with a root mean square error (RMSE) of around 8.6×10^{-4}.

The number of membership functions (MF) was set to 15 following a sensitivity analysis. This value was identified as the optimal trade-off, minimizing the Root Mean Square Error (RMSE) during the training phase without inducing overfitting or excessive computational load. Furthermore, triangular membership functions were selected over Gaussian or trapezoidal shapes. Their linear mathematical formulation requires fewer arithmetic operations compared to the exponential calculations of Gaussian functions, making them significantly more efficient for implementation in real-time control loops.

The FL controller design method is detailed in (Lorenzo et al., 2017) (Stitou et al., 2023). To ensure effective tracking, the Fuzzy Logic Controller (FLC) processes two inputs: the error E and the change of error ΔE. These are defined in equations (1) and (2), where V_{mpp} is the reference voltage at the Maximum Power Point and E_p is the error at the previous sampling instant.

$$E(k) = V_{mpp}(k) - V_{in}(k) \quad (1)$$

$$\Delta E(k) = E(k) - E_p(k) \quad (2)$$

The rule base presented in Table 2 was designed using a heuristic approach to mimic the behaviour of a non-linear PI controller: large errors trigger aggressive duty cycle adjustments to ensure fast convergence, while small errors result in fine-tuning to minimize steady-state oscillations. To adapt these normalized rules to the physical system, scaling factors are applied to the inputs (K_e, K_{de}) and the output (K_{dD}). These parameters were determined through an iterative process (trial and error) to optimize the response time and stability. The final tuned values used in this simulation are: $K_e = \frac{1}{300}$, $K_{de} = \frac{1}{300}$ and $K_{dD}=0.1$.

The membership functions for the input variables are illustrated in Fig. 6 and Fig. 7, while Fig. 8 shows the membership functions for output. The interpretation used for the rules is Mandani, and the Defuzzification used is Centroid (Mudzakir et al., 2021). On completion of the design, the controller is implemented in Simulink, as shown in Fig.9.

Table 2 Rules for error and error variation.

		Error Variation				
		NB	**NS**	**Z**	**PS**	**PB**
Error	**NB**	NB	NB	NB	NS	Z
	NS	NB	NB	NS	Z	PS
	Z	NS	NS	Z	PS	PB
	PS	NS	Z	PS	PB	PB
	PB	Z	PS	PB	PB	PB

Where:
PB: Positive big; PS: Positive small; Z: Zero; NS: Negative small; NB: Negative big
The proposed FLC utilizes triangular membership functions (MFs) for both inputs and output due to their computational efficiency. The universe of discourse for the inputs (E, ΔE) and output (D) is normalized between [-1, 1]. To ensure smooth control transitions, the MFs are designed with a 50% overlap between adjacent sets (e.g., 'Zero' overlaps with 'Positive Small' and 'Negative Small'). This overlap is crucial for eliminating dead zones and ensuring continuous control action. The specific tuning of the scaling factors (K_e, K_{de}, K_{dD}) adapts these normalized ranges to the physical system dynamics."

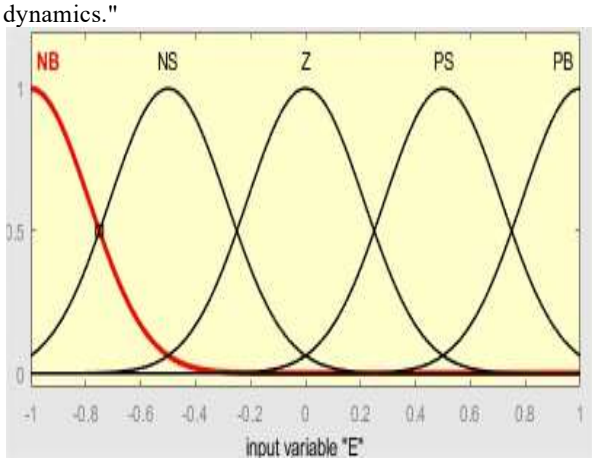

Fig. 6 MF plots of error

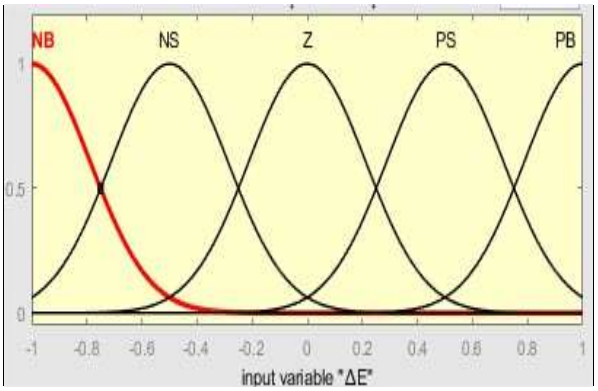

Fig. 7 MF plots of error variation.

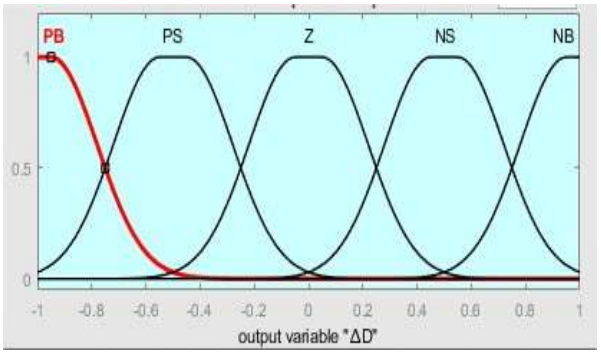

Fig. 8 MF plots of duty ratio.

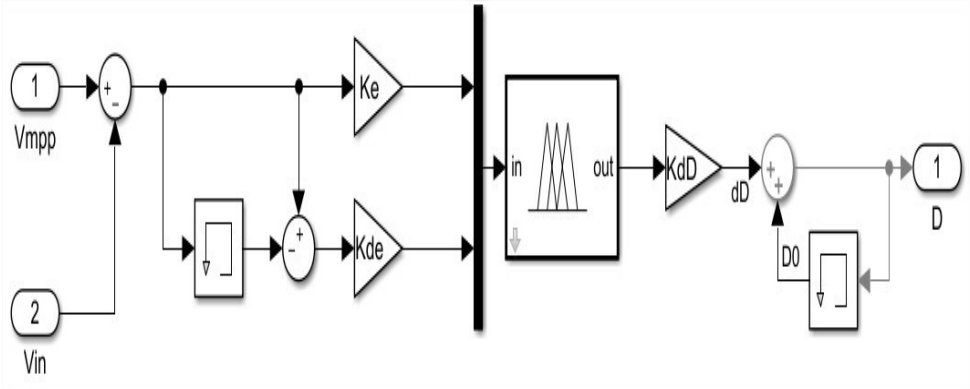

Fig. 9 FL controller implementation

MATLAB Simulink was used to implement the control, based on the system components presented above. The simulation of the MPPT controller is shown in Fig.10.

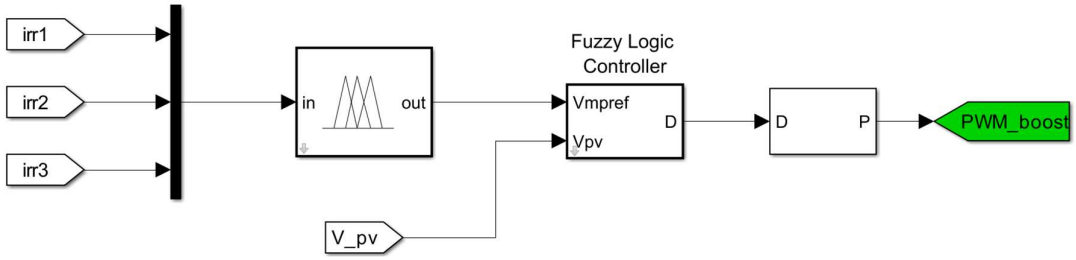

Fig. 10 ANFIS-FL MPPT implementation

B. DC Bus Voltage Regulation

The boost converter output delivers DC voltage, while the load requires a three-phase AC power supply. This conversion requires the use of an inverter. In addition to its main function of converting DC voltage to AC voltage, the inverter also plays a crucial role in regulating the DC bus voltage (Li et al., 2021). By adjusting its control signals, it helps maintain a stable voltage on the DC bus. These two functions are essential to ensure overall system performance, as well as the quality and stability of the power supplied to the load (Mourouvin et al., 2021).

A universal bridge inverter, based on IGBT-diodes, has been implemented using the MATLAB/Simulink library to meet these requirements. This model is illustrated in Fig.11.

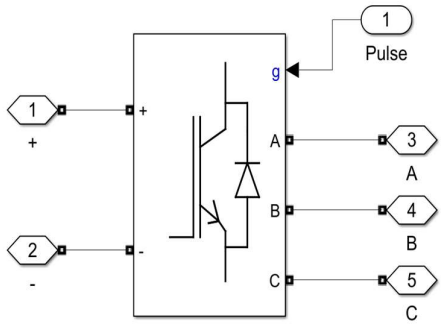

Fig. 11 Universal bridge inverter

Constant DC bus voltage enables AC voltage to be produced with stable amplitudes, thus optimizing the quality of the load supply. On the other hand, any fluctuation in DC voltage can lead to undesirable variations in the AC voltage supplied, compromising system stability and efficiency, and even causing overall malfunction (Mohammed and Jung, 2021).

The DC bus voltage was set to 800V. This value is justified by the fundamental operation of three-phase SPWM inverters to ensure linear modulation. according to (Rashid, 2014), the relationship between the DC link voltage and the Line-to-Line RMS output voltage ($V_{LL,rms}$) in the linear modulation region (amplitude modulation index $m_a < 1$) is given by (3):

$$V_{LL,rms} = \frac{\sqrt{3}}{2\sqrt{2}} m_a V_{dc} \quad (3)$$

For a standard grid integration or load requirement, a DC bus of 800 V allows the inverter to synthesize the required AC voltage while keeping m_a in the linear range, thus avoiding overmodulation and minimizing harmonic distortion.

To regulate DC bus voltage, we have adopted vector control of a Voltage Source Converter (VSC) (Irnawan et al., 2024). Vector control is an advanced method of electrical power control that enables independent and instantaneous control of active and reactive currents through the use of the synchronously rotating dq reference frame. This method relies on coordinate transformations (Clark and Park) to convert three-phase variables into a rotating reference frame (Shang et al., 2024). Precise control requires synchronization via a PLL (phase-locked loop), which calculates the angle required to decouple the active and reactive components. The vector control system uses internal and external loops: the internal loop manages power exchanges between the DC bus and the load, while the external loop regulates the DC bus voltage. The control signals are then transformed into three-phase voltages to drive the switching devices via PWM (Huang et al., 2015).

In our configuration, the reactive component iq is zero, as a resistive load does not require reactive power. One of the main reasons for choosing vector control lies in our long-term vision for the project, which includes the possibility of injecting the energy generated directly into the power grid. Vector control offers the flexibility and precision needed to independently control active and reactive power, an essential capability for grid injection (Atillah et al., 2024). It stabilizes and optimizes energy flow by adapting to grid conditions, facilitating a future transition to a grid-interconnected energy management system.

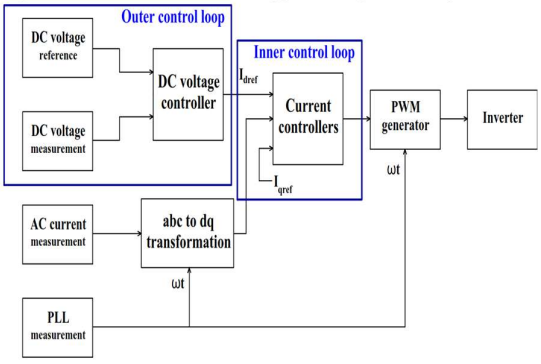

Fig. 12 Vector control principle

The control was implemented using MATLAB Simulink, as is shown in Fig.13.

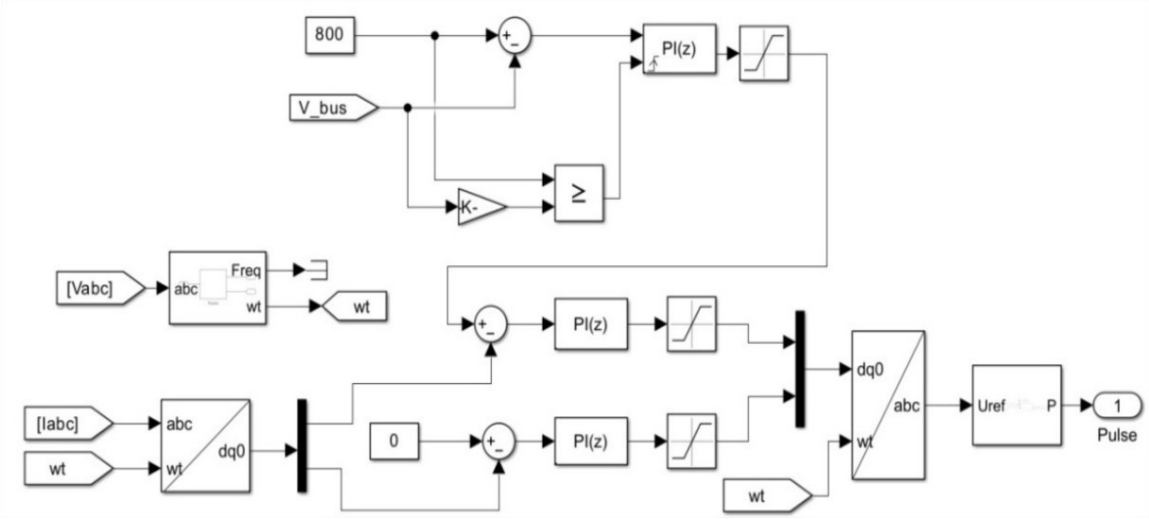

Fig. 13 Vector control implementation

C. Storage system

Storage systems play an essential role in managing the intermittent nature of solar energy, which is not always available. To compensate for this variability, capturing and storing the excess energy produced during high solar panel production is crucial. The approach adopted is to capitalize on these promising moments to store excess energy, after satisfying load power requirements (El Mezdi et al., 2023).

A bi-directional buck-boost converter has been integrated to ensure battery safety during charging and discharging, as shown in Fig.14 (Mbungu et al., 2020). This converter is complemented by a dedicated controller, shown in Fig.15. Together, they play an essential role in energy management, regulating exchanges between the battery, the solar panels, and the load (Rathor and Saxena, 2020) .

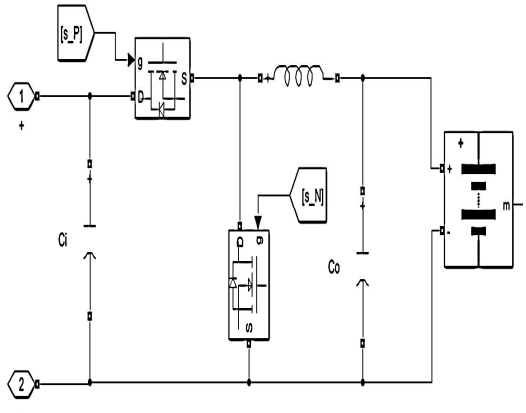

Fig. 14 Bi-directional buck-boost converter

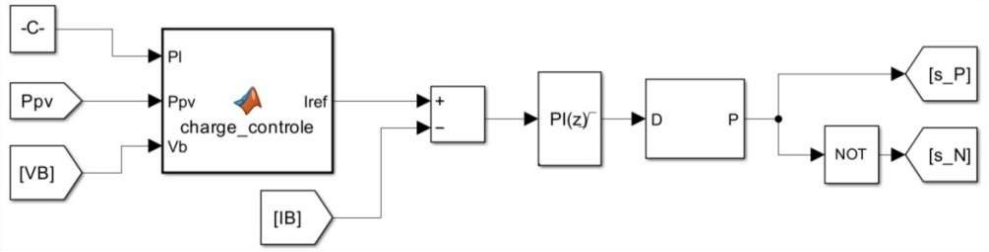

Fig. 15 Charging-discharging control

Our proposed algorithm, describing how the battery controller works, is illustrated in Fig.16. The main aim of this algorithm is to control the battery's charging and discharging power by regulating its current (IB). To do this, the algorithm calculates the reference current (Iref) based on the difference between the power demanded by the load (PL) and the power supplied by the photovoltaic panels (PPV). This difference is then compared with the maximum permissible battery power (PBmax). Based on this comparison, the algorithm determines whether the battery should be charged or discharged, and calculates the current Iref corresponding to the charging or discharging power, considering the battery voltage (VB). This dynamic management ensures an optimum balance between energy production, consumption, and storage while respecting the battery's operational limits.

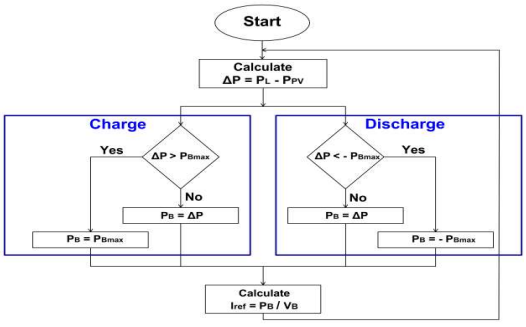

Fig. 16 Charging-discharging algorithm

It is important to note that for the purpose of this simulation, which focuses on the MPPT tracking dynamics over a short timeframe, the battery is assumed to operate within its nominal State of Charge window (20% < SoC < 95%). Consequently, the simplified logic presented here prioritizes power balance. In a long-term implementation, this algorithm would naturally include strict cut-off layers to disable charging when SoC > 95% and halt discharging when SoC < 20% to prevent deep discharge cycles, ensuring the longevity of the storage unit.

D. Excess Power Management

When PV panel production exceeds both the load demand and the maximum battery charging capacity, the system must evacuate the surplus energy to maintain the DC bus voltage stability at 800V.

In this simulation, this evacuation system is modelled as a controlled active power sink. Although represented in the schematic as a variable load for modelling purposes, as shown in Fig.17, this block acts as a theoretical equivalent to a Dump Load Controller. In a physical implementation of an off-grid system, this surplus energy is not merely wasted as heat in a rheostat. Instead, it is diverted to non-priority resistive loads (deferrable loads) to valorise the excess production, such as:

- Resistive Heating: Water heaters or space heating systems.
- Water Pumping: Storing potential energy in reservoirs.
- Grid Injection: Feeding a neighboring microgrid (in future interconnected scenarios).

The control algorithm detailed in Fig.18. determines the exact amount of power (ΔP') that needs to be removed from the DC bus. The equivalent resistance value (R) is computed dynamically in the simulation to act as a load matching this surplus.

This approach allows for the validation of the system's power balance capability. It ensures that the excess energy is effectively managed simulating its valorisation through auxiliary tasks rather than allowing a dangerous DC bus overvoltage to occur

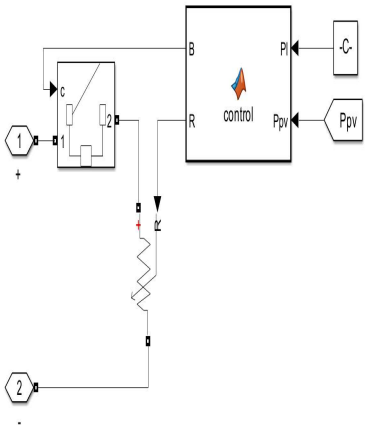

Fig. 17 Dissipating excess energy system

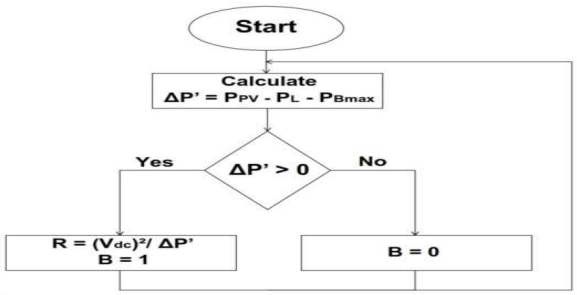

Fig. 18 Dissipating excess energy algorithm

where V_{dc} is the DC Bus Voltage, R is the Resistance Value, and B the Breaker Command.

III. RESULTS AND DISCUSSION

In this section, the evaluation of the system and studied algorithms in terms of power balance will be conducted. Specifications for the various system components are calculated based on the methods presented in (Atillah et al., 2023). Are shown in Table 3. The selected specifications of the battery are used exclusively to check the algorithm's performance and are not based on any particular dimensioning. For the initial state of charge of the battery, a state of 50% is supposed to limit the study. Future work could consider fully charged and discharged battery cases. To isolate the performance of the proposed control strategy, the following assumptions were made during the simulation:

- Simulation Profile: The simulation is conducted over a total duration of 18 seconds, divided into three distinct intervals. Between these intervals, the solar irradiance profile undergoes quasi-instantaneous variations (steep ramps) rather than gradual changes. This configuration is intentionally designed to simulate extreme dynamic scenarios.
- Thermal Modeling: The thermal behavior of the battery and power converters is not included in this study. The components are assumed to operate at a constant ambient temperature of 25°C, and the internal resistance of the battery is considered constant during charge/discharge cycles.
- Converter Efficiency: The DC-DC and DC-AC converters are modeled using ideal switches (IGBT/Diodes) within the MATLAB/Simulink environment. Consequently, switching and conduction losses are neglected to focus primarily on the validation of the logic control algorithms.
- Load Characteristics: The load is modelled as a balanced three-phase resistive system. This ensures symmetrical current consumption across phases and eliminates reactive power considerations, allowing for a clear assessment of the active power management capability.

Table 3 System specifications

PV (1000 W/m²)	Boost converter	Buck-Boost converter	Battery
Ppv max: 50 KW Vpv max: 415 V Ipv max: 120.5 A	Input capacitor: 100 µF Output capacitor: 1 mF Inductance: 9.6575 mH Switching frequencie: 2 KHz	Input capacitor: 1 mF Output capacitor: 10 µF Inductance: 130 mH Switching frequencie: 2 KHz	Type: lithium-ion Capacity: 150 Ah Maximum power: 10 KW

The DC-AC inversion stage is modelled using the 'Universal Bridge' block (IGBT/Diode) within MATLAB/Simulink. The control signals are generated using a carrier-based two-level PWM method with a switching frequency set to 5 KHz.

Concerning the irradiance, the profile used is shown in Fig.19.

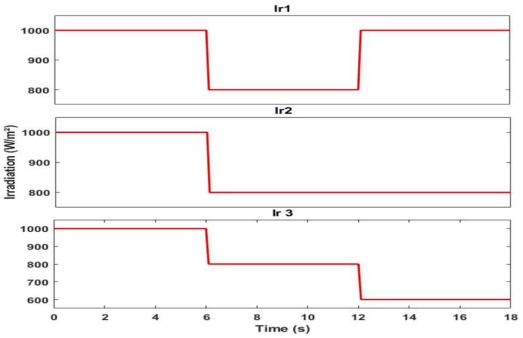

Fig. 19 Irradiation profile used

During the first 6 seconds, the three PV panels receive an irradiation of 1000 W/m². According to the power curve in Fig.3 (a), the system should deliver around 50 KW. Between the 6th and 12th seconds, irradiation decreases to 800 W/m² for all three panels, corresponding to a power output of around 40 KW. Finally, during the last 6 seconds, to simulate a partial shading scenario, the panels receive three different levels of irradiation: 1000 W/m², 800 W/m², and 600 W/m², with an expected overall power of around 33 KW, as shown on the power curve in Fig.3 (b).

The simulations are designed to analyze various energy flow management scenarios involving solar panels, batteries, loads, and evacuation systems. Two load powers will be considered for these simulations: 35 KW and 40 KW.

A. Load power demand of 35 KW

When the load requires a constant power of 35 KW, the system operates and performs as follows.

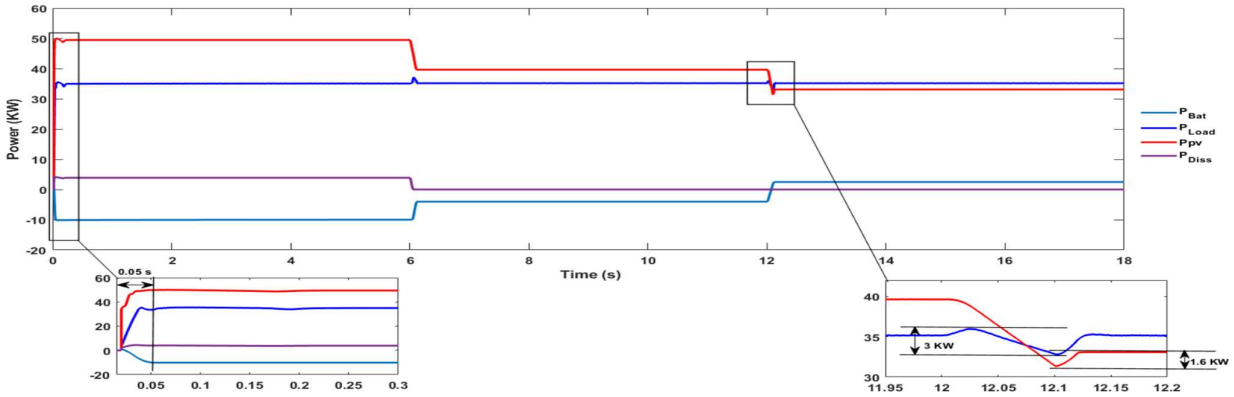

Fig. 20 Various power curves

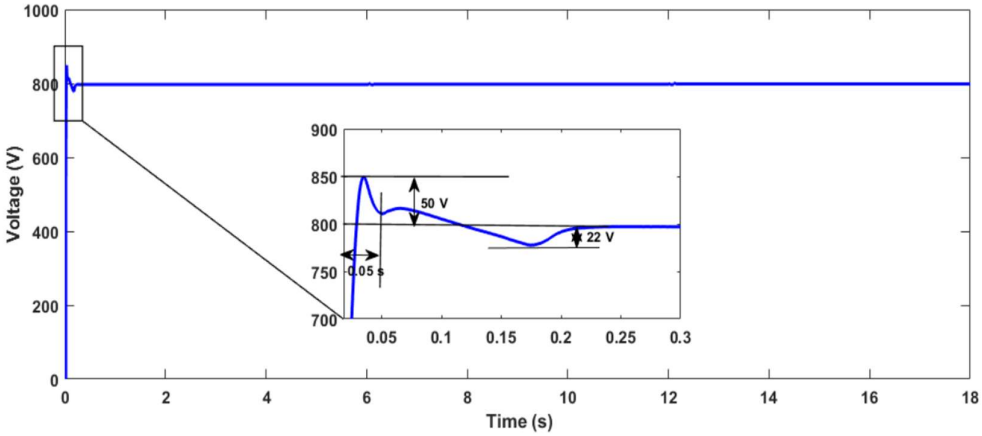

Fig. 21 DC Bus Voltage curve

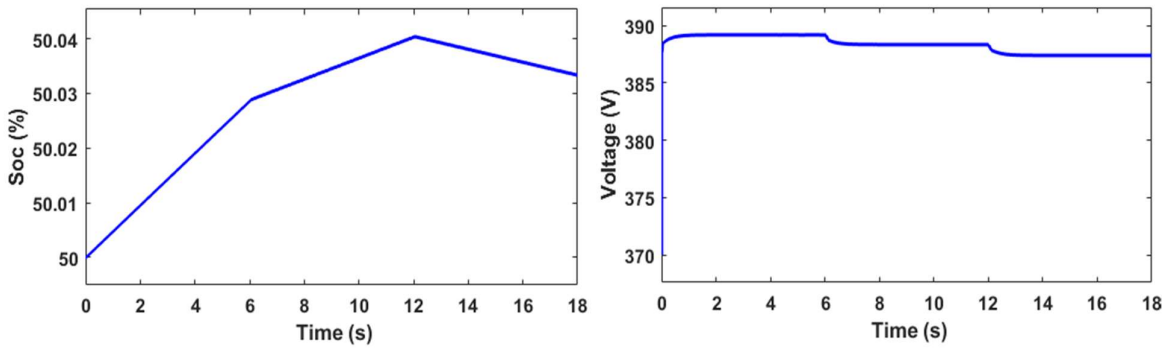

(a) (b)

Fig. 22 (a) Battery state of charge (b) Battery voltage

1) ANFIS-FL MPPT control performance

The performance of the proposed MPPT control, based on ANFIS and FL, was evaluated for its ability to extract the maximum available power from the PV panels under different irradiation conditions.

First, during the first 6 seconds, the panels were subjected to a uniform irradiation of 1000 W/m². The control was able to extract a power of around 50 KW, as shown in Fig.20, which corresponds exactly to the maximum power the panels can deliver under these conditions.

Then, when irradiance fell to 800 W/m² over the next 6 seconds, the control adapted quickly and extracted power of 40 KW, in line with the theoretical performance of panels.

To simulate partial shading conditions, the panels were subjected to three different irradiation levels over the last 6 seconds: 600 W/m², 800 W/m², and 1000 W/m². Despite this irregular irradiance distribution, the MPPT control was able to extract a power output of 33 KW, as shown in Fig.20, corresponding to the maximum power available under these conditions.

Beyond the final power extraction value, the dynamic behaviour of the extracted power (P_{PV}), visible in the zoomed insets of Fig. 20, provides critical insight into the MPPT tracking quality. Unlike conventional P&O algorithms that often exhibit power ripples around the optimal point, the ANFIS-FL controller drives the power monotonically toward the theoretical maximum (50 KW) with a settling time of 0.05 s. The absence of power oscillation around the steady-state value confirms that the operating voltage is locked precisely onto the P-V curve peak (V_{mpp}), ensuring stability without hunting losses.

These results confirm the accuracy and efficiency of MPPT control based on ANFIS and FL, whether under conditions of uniform irradiation or partial shading. Fig.21 also highlights the stability of the control and its ability to quickly follow the maximum power point, regardless of irradiation variations.

2) Managing storage and dissipating excess energy

The second part of this study concerns the efficiency of storage management algorithms and the dissipation of excess electrical energy, aimed at balancing production and consumption while guaranteeing constant availability of the power required by the load.

In this scenario, the load requires a constant power of 35 KW. During the first 6 seconds, when the PV panels are producing 50 KW of power, an excess of 15 KW is observed. Since the maximum charging power of the battery is limited to 10 KW, this excess is managed in a balanced way: 10 KW is directed to the battery for storage, while the remaining 5 KW is dissipated in a variable resistor connected to the DC bus, as shown in Fig.22.

Between 6th and 12th seconds, when the panels deliver 40 KW, a surplus of 5 KW is present. This surplus is directed entirely to the battery, which continues to charge. During this period, the dissipation device remains inactive, demonstrating optimized management of the available energy.

Finally, for the last 6 seconds, the PV panels produce 33 KW less than the load demand. In this case, a deficit of 2 KW is made up by the battery, guaranteeing continuous supply to the load. During this phase, the dissipation device also remains inactive, as no excess energy is generated.

Battery Dynamics Analysis: To validate the internal behaviour of the storage unit, the Battery Voltage (V_{bat}) and State of Charge (SoC) evolution are presented in Fig.22.

- Voltage: The voltage remains stable around the nominal value. The observable step changes correspond to the physical voltage drop/rise across the internal resistance ($\Delta V = R_{int}*\Delta I$) triggered by the switching between charging and discharging modes.
- SoC: The SoC evolution validates the energy integration. The positive slope during the first 6s corresponds to the charging phase (excess power), while the negative slope during shading (12-18s) confirms discharging to support the load.
- Current: Note that the Battery Power (P_B) curve in Fig. 20 serves as a direct proxy for the current dynamics ($I_{bat} \approx P_B / V_{nom}$), demonstrating the instantaneous response.

3) DC bus regulation performance

A critical point in the study was the system's ability to keep the DC bus voltage stable, regardless of variations in production or consumption. The DC bus voltage is regulated at a constant value of 800 V, irrespective of operating conditions or dynamic changes in irradiation levels and loads.

As shown in Fig.21, this stability is guaranteed throughout the various simulated phases, including transitions between periods of energy surplus, storage, or battery compensation.

4) Analysis of Transient Overshoot in Power and Voltage

The curves shown in Fig.20 and Fig.21 representing the power supplied by the photovoltaic panels, consumed by the load, and the DC bus voltage show certain overshoots during transient regimes, whether at process start-up or during irradiation changes. These overshoots can potentially cause problems for the system, notably by affecting stability or causing damage to components. An analysis was carried out to assess the danger of these overshoots. This involves measuring the amplitude and duration of the most significant overshoots visible on the curves. These parameters are used to determine whether the overshoots are within acceptable limits.

The most noticeable transient overshoot occurs during the change in irradiation from 800 W/m² to 600 W/m². During this transition, the load power exhibits an overshoot of 3 KW throughout 0.1 s, representing 8.75% of the nominal power. This value remains below the 10% threshold, and the short duration minimizes its impact on the system's stability and reliability.

Similarly, under the 40 KW load scenario, the DC bus voltage curve exhibits a transient overshoot reaching 872 V. While a 9% deviation warrants attention, it remains well within the Safe Operating Area (SOA) of standard industrial components designed for 800 V DC bus topologies. According to standard power electronics design rules (Rashid, 2014), such systems typically utilize 1200 V rated IGBTs and capacitors to withstand switching spikes. Consequently, a peak voltage of 872 V utilizes only ~73% of the component breakdown voltage, leaving a safety margin of over 300 V. Therefore, the observed overshoot poses no risk of component failure in a real-world implementation.

B. Load power demand of 40 KW

When the load requires a constant power of 40 KW, the system operates and performs as follows:

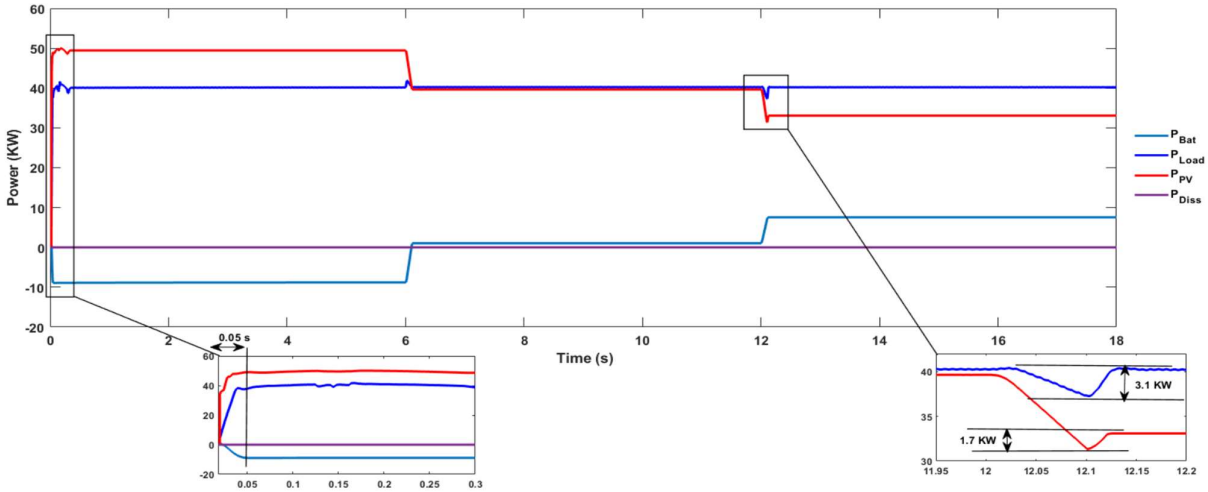

Fig. 23 Various power curves

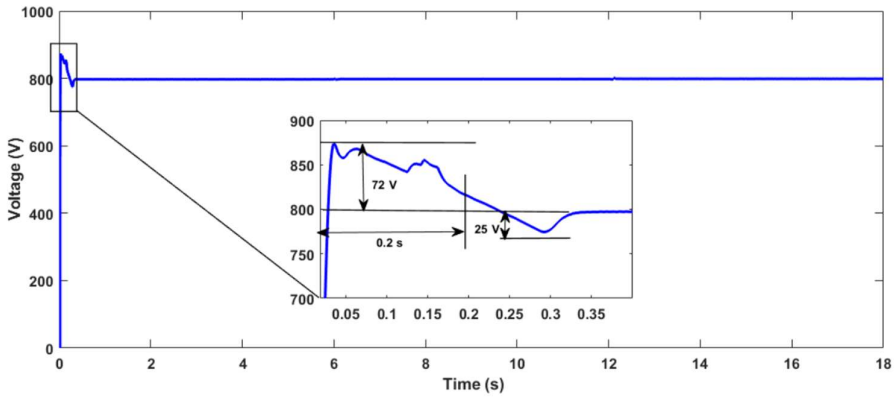

Fig. 24 DC Bus Voltage curve

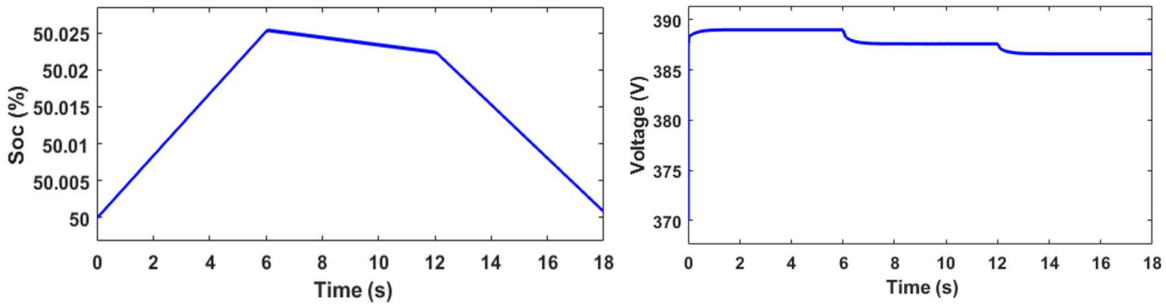

(a) (b)

Fig. 25 (a) Battery state of charge (b) Battery voltage

1) ANFIS-FL MPPT control and DC bus regulation performance

As in the first scenario, MPPT control based on ANFIS and FL has proven effective in maximizing power extraction from the panels in uniform conditions and under partial shading. As for DC bus voltage regulation, Fig.24 shows that it remains stable at 800 V, irrespective of irradiation variations and panel output, guaranteeing optimal system operation.

2) Managing storage and dissipating excess energy

In this scenario, the load is supposed to require a constant power of 40 KW. Fig.24 shows that when the panels produce around 50 KW, an excess of around 10 KW is directed to the batteries. When the power supplied by the panels is slightly less than the load demand, this small difference is compensated for by the batteries. In partial shading conditions, when the panels deliver around 33 KW, the batteries provide around 7 KW. It's important to note that, during this scenario, the excess dissipation system remains inactive throughout the entire period.

Battery Dynamics Analysis: Similarly, for the 40 KW scenario, the battery dynamics shown in Fig.25 confirm the consistency of the management algorithm under heavier load conditions. The SoC profile adapts correctly to the higher demand, with a steeper discharging slope compared to the 35 KW case. As in the previous scenario, the voltage stability and the perfect correlation between the SoC slope and the power flow direction validate the robustness of the proposed EMS.

3) Analysis of Transient Overshoot in Power and Voltage

In the second scenario, as shown in Fig.24, the load power exhibits a transient overshoot of 3.1 KW lasting 0.1 s during irradiation changes, corresponding to 7.75% of the nominal power.

In Fig.24, the DC bus voltage reaches a peak of 872 V, exceeding the nominal value of 800 V by 9%, over approximately 0.2 s. While these overshoots are slightly more pronounced than in the first scenario, they remain within manageable limits, ensuring the overall system's stability and reliability.

C. Quantitative Performance and Comparative Analysis

To provide a rigorous assessment beyond qualitative observations, the system's performance was analysed using key statistical metrics: response time, steady-state stability, and power extraction capability. The proposed ANFIS-FL hybrid controller demonstrates consistent robustness across both load scenarios (35 KW and 40 KW):

- Response Time: The controller achieves a rapid settling time of 0.05 s for both start-up and sudden irradiance changes. This speed is maintained regardless of the load demand.
- Tracking Efficiency: Instead of oscillating around the optimal point, the proposed ANFIS-FL controller demonstrates near-ideal tracking efficiency. As observed in the results, the extracted power converges exactly to the theoretical maximums (50 KW, 40 KW, and 33 KW) with negligible steady-state error, confirming the maximization of energy harvesting.
- Steady-State Stability: Once the MPP is reached, the power oscillation is negligible, contrasting with the continuous ripple often observed in conventional methods.

To further contextualize these results, we compare the proposed method with standard algorithms analysed in a prior comparative study (Atillah et al., 2024), specifically Perturb & Observe (P&O), Particle Swarm Optimization (PSO), and ANN-based controllers.

Conventional methods like P&O typically face a fundamental trade-off: a small step size reduces oscillations but slows down tracking (often >0.1s), while a large step size speeds up tracking but increases power loss due to steady-state ripple. Furthermore, under partial shading conditions, P&O often gets trapped in local maxima.

The proposed ANFIS-FL approach eliminates these limitations. It achieves 0.05s convergence significantly faster than the iterative process required by PSO or the settling time of standard P&O while maintaining stability

without oscillations. Unlike PSO, which requires a high computational burden to scan for the Global MPP, the proposed algorithm successfully identifies the Global MPP (33 KW) instantly without hesitation, combining the speed of direct control with the global search capability of meta-heuristic methods.

The comparison between the 35 KW and 40 KW scenarios confirms the decoupling capability of the control strategy. Although the DC bus voltage overshoot increased slightly under heavier load, the MPPT tracking time remained identical at 0.05 s. This confirms that the energy management system effectively isolates the solar generation side from load-side disturbances.

IV. CONCLUSION

This study successfully validated a holistic control framework for standalone photovoltaic systems, addressing the critical challenge of maintaining transient stability under dynamic partial shading conditions.

The simulation results demonstrate that the proposed ANFIS-FL hybrid controller effectively eliminates the classic trade-off found in conventional algorithms (like P&O) between tracking speed and steady-state accuracy. The system achieved a settling time of 0.05 s with zero steady-state oscillation, ensuring distinct Global MPP tracking (reaching 33 KW under severe shading) where standard methods typically falter. Furthermore, the analysis of the DC bus dynamics confirmed that despite transient overshoots (peaking at 872 V), the system remains well within the safe operating area of standard 1200 V industrial hardware.

The primary contribution of this work is the demonstration of a robust decoupling capability. The control strategy successfully isolates the PV generation dynamics from the load-side disturbances (35 KW vs. 40 KW scenarios). This proves that an intelligent neuro-fuzzy approach can secure the stability of a fully integrated off-grid chain comprising storage and excess management without the computational burden of population-based meta-heuristics.

While the robustness of the control logic is confirmed, this study relied on a simplified "Dump Load" model (variable resistor) and assumed nominal battery temperature. Future research will focus on two specific axes:

- Smart Load Valorization: Replacing the dissipation unit with actively controlled deferrable loads (e.g., water heating or pumping) to improve the overall system exergy efficiency.
- Grid Interconnection: Evolving the current off-grid topology into a grid-tied microgrid architecture, allowing the surplus power to be injected into the utility grid rather than dissipated.

AUTHOR CONTRIBUTIONS

All authors have made a substantial, direct, and intellectual contribution to the work.

REFERENCES

Aghdam, A. D., N. J. Dabanloo, F. N. Rahatabad, K. Maghooli (2024). Design and Stability Analysis of an Adaptive Neuro-Fuzzy Inference System (ANFIS)-Based Pacemaker Controller in MATLAB Simulink. *Journal of Long-Term Effects of Medical Implants,* 34(4).

Assem, H., T. Azib, F. Bouchafaa, C. Laarouci, N. Belhaouas, A. Hadj Arab (2023). Adaptive Fuzzy Logic-Based Control and Management of Photovoltaic Systems with Battery Storage. *International Transactions on Electrical Energy Systems,* 2023(1), 9065061.

Atillah, M. A., H. Stitou, A. Boudaoud, M. Aqil (2023). Performance analysis of three MPPT controls under partial shading: P&O, PSO and ANN. *E3S Web of Conferences,* 469, 00064.

Atillah, M. A., H. Stitou, A. Boudaoud, M. Aqil (2024). Comparative Study of Two ANFIS-Based MPPT Controls under uniform and partial shading conditions. *Solar Energy and Sustainable Development Journal,* 89–103.

Atillah, M. A., H. Stitou, A. Boudaoud, M. Aqil, A. Hanafi (2024). Study and analysis of partial shading effect on power production of a photovoltaic string controlled by three different MPPT techniques: P&O, PSO and ANN. *Mathematical Modeling and Computing,* 11(3), 856–869.

Atillah, M. A., H. Stitou, A. Boudaoud, M. Aqil (2024). Power Flow Management for Off-Grid Photovoltaic-Battery System Using ANN-FL Controller MPPT. In *International Conference on Connected Objects and Artificial Intelligence* (pp. 158–164). Springer Nature Switzerland.

Çakmak, F., Z. Aydoğmuş, M. R. Tür (2025). Analyses of PO-Based Fuzzy Logic-Controlled MPPT and Incremental Conductance MPPT Algorithms in PV Systems. *Energies,* 18(2), 233.

Chapala, S., R. L. Narasimham, G. R. Das (2024). Power Quality Analysis of ANFIS Based Distributed Generation System with UPQC. *International Journal of Engineering and Manufacturing,* 14(4), 1–14.

Chtita, S., A. Derouich, A. El Ghzizal, S. Motahhir (2021). An improved control strategy for charging solar batteries in off-grid photovoltaic systems. *Solar Energy,* 220, 927–941.

El Mezdi, K., A. El Magri, A. Watil, I. El Myasse, L. Bahatti, R. Lajouad, H. Ouabi (2023). Nonlinear control design and stability analysis of hybrid grid-connected photovoltaic-Battery energy storage system with ANN-MPPT method. *Journal of Energy Storage,* 72, 108747.

Farah, L., A. Haddouche, A. Haddouche (2020). Comparison between proposed fuzzy logic and ANFIS for MPPT control for photovoltaic system. *International Journal of Power Electronics and Drive Systems,* 11(2), 1065.

Ghizlane, C., B. Mohcine, B. Abdenabi, A. Abdelouahed (2024). Performance analysis of MPPT tracking algorithm based on artificial neural network for a PV pumping system. In *2024 4th International Conference on Innovative Research in Applied Science, Engineering and Technology (IRASET)* (pp. 1–7). IEEE.

Huang, Y., X. Yuan, J. Hu, P. Zhou, D. Wang (2015). DC-bus voltage control stability affected by AC-bus voltage control in VSCs connected to weak AC grids. *IEEE*

Journal of Emerging and Selected Topics in Power Electronics, 4(2), 445–458.

Irnawan, R., R. F. Mochamad, F. F. da Silva, Q. Zhang, Sarjiya, C. L. Bak, E. Haryadi (2025). Review of HVDC technologies for weak grid interconnectors. *Electrical Engineering,* 107, 4483–4501.

Kelly, E., B. A. M. Nouadje, R. H. T. Djiela, P. T. Kapen, G. Tchuen, R. Tchinda (2023). Off-grid PV/Diesel/Wind/Batteries energy system options for the electrification of isolated regions of Chad. *Heliyon,* 9(3).

Khan, M., M. A. Raza, T. A. Jumani, S. Mirsaeidi, A. Ali, G. Abbas, A. Alshahir (2023). Modeling of intelligent controllers for solar photovoltaic system under varying irradiation conditions. *Frontiers in Energy Research,* 11, 1288486.

Li, C., Y. Cao, Y. Yang, L. Wang, F. Blaabjerg, T. Dragicevic (2021). Impedance-based method for DC stability of VSC-HVDC system with VSG control. *International Journal of Electrical Power & Energy Systems,* 130, 106975.

Lorenzo, J., J. C. Espiritu, J. Mediavillo, S. J. Dy, R. B. Caldo (2017). Development and implementation of fuzzy logic using microcontroller for buck and boost DC-to-DC converter. *IOP Conference Series: Earth and Environmental Science,* 69(1), 012193.

Mbungu, N. T., R. M. Naidoo, R. C. Bansal, M. W. Siti, D. H. Tungadio (2020). An overview of renewable energy resources and grid integration for commercial building applications. *Journal of Energy Storage,* 29, 101385.

Mohammed, A. N., S. Umar, S. Chatterjee (2024). ANFIS systematic robustness investigation for AVR system. *e-Prime – Advances in Electrical Engineering, Electronics and Energy,* 9, 100670.

Mohammed, H. A., R. Mohd-Mokhtar, H. I. Ali (2025). An optimal adaptive neuro-fuzzy inference system for photovoltaic power system optimization under partial shading conditions. *Energy Systems,* 1–24.

Mohammed, S. A. Q., J. W. Jung (2021). A state-of-the-art review on soft-switching techniques for DC–DC, DC–AC, AC–DC, and AC–AC power converters. *IEEE Transactions on Industrial Informatics,* 17(10), 6569–6582.

Mokhtara, C., B. Negrou, N. Settou, B. Settou, M. M. Samy (2021). Design optimization of off-grid Hybrid Renewable Energy Systems considering the effects of building energy performance and climate change: Case study of Algeria. *Energy,* 219, 119605.

Mourouvin, R., J. C. Gonzalez-Torres, J. Dai, A. Benchaib, D. Georges, S. Bacha (2021). Understanding the role of VSC control strategies in the limits of power electronics integration in AC grids using modal analysis. *Electric Power Systems Research,* 192, 106930.

Mudzakir, M. A., A. Marwanto, S. Alifah (2021). Boost Buck Converter Based on Fuzzy Logic for Voltage Stabilizer. *Journal of Telematics and Informatics,* 9(1), 1–11.

Rad, M. A. V., A. Kasaeian, X. Niu, K. Zhang, O. Mahian (2023). Excess electricity problem in off-grid hybrid renewable energy systems: A comprehensive review from challenges to prevalent solutions. *Renewable Energy,* 212, 538–560.

Rashid, M. H. (2014). *Power Electronics: Circuits, Devices, and Applications* (4th ed.). Pearson Education.

Rathor, S. K., D. Saxena (2020). Energy management system for smart grid: An overview and key issues. *International Journal of Energy Research,* 44(6), 4067–4109.

Seguel, J. L., S. Zenteno, C. Arancibia, J. Rodríguez, M. Aly, S. I. Seleme Jr., L. M. Morais (2025). An Enhanced Solar Battery Charger Using a DC-DC SEPIC Converter and Fuzzy Logic-Based Control for Off-Grid Photovoltaic Applications. *Processes,* 13(1), 99.

Shang, L., Z. Hua, X. Dong, Y. Tian (2023). Vector synchronization stabilizer to enhance small-signal stability of VSC-dominant power system in DC-voltage control timescale. *CSEE Journal of Power and Energy Systems.*

Stitou, H., M. A. Atillah, A. Boudaoud, M. Aqil (2024). Load forecasting using fuzzy logic, artificial neural network, and adaptive neuro-fuzzy inference system approaches: application to South-Western Morocco. *International Journal of Electrical & Computer Engineering,* 14(6).

Stitou, H., M. A. Atillah, A. Boudaoud, A. Mounaim (2023). Medium-term load forecasting using fuzzy logic approach: A case study of Taroudannt province. *E3S Web of Conferences,* 469, 00063.

Timur, O., B. K. Uzundağ (2025). Design and Analysis of a Hybrid MPPT Method for PV Systems Under Partial Shading Conditions. *Applied Sciences,* 15(13), 7386.

Yatimi, H., Y. Ouberri, S. Chahid, E. Aroudam (2020). Control of an off-grid PV system based on the backstepping MPPT controller. *Procedia Manufacturing,* 46, 715–723.

Zhang, Y., Y. Zhang (2019). An advanced digital predictive valley current control algorithm for a boost converter. *Journal of Physics: Conference Series,* 1207(1), 012001.